Environ. Sci. Technol. **2004**, *38,* 6809–6816

Development and Application of a Mobile Laboratory for Measuring Emissions from Diesel Engines. 2. Sampling for Toxics and Particulate Matter

DAVID R. COCKER III,*,†,‡
SANDIP D. SHAH,†,‡ KENT C. JOHNSON,‡
XIAONA ZHU,†,‡ J. WAYNE MILLER,‡ AND
JOSEPH M. NORBECK†,‡

Department of Chemical and Environmental Engineering,
Bourns College of Engineering, and
Bourns College of Engineering Center for Environmental
Research and Technology, University of California,
Riverside, California 92521

Limited data are available on the emission rates of speciated volatile and semivolatile organic compounds, as well as the physical and chemical characteristics of fine particulate matter (PM) from mobile, in-use diesel engines operated on the road. A design for the sampling of these fractions and the first data from in-use diesel sources are presented in this paper. Emission rates for carbonyls, 1,3-butadiene, benzene, toluene, xylene, PM, and elemental and organic carbon (EC and OC) are reported for a vehicle driven while following the California Air Resources Board (ARB) four-mode heavy heavy-duty diesel truck (HHDDT) cycle and while transiting through a major transportation corridor. Results show that distance specific emission rates are substantially greater in congested traffic as compared with highway cruise conditions. Specifically, emissions of toxic compounds are 3–15 times greater, and PM is 7 times greater under these conditions. The dependence of these species on driving mode suggests that health and source apportionment studies will need to account for driving patterns in addition to emission factors. Comparison of the PM/NO_x ratios obtained for the above tests provides insight into the presence and importance of "off-cycle" emissions during on-road driving. Measurements from a stationary source (operated and tested at constant engine speed) equipped with an engine similar to that in the HHDDT yielded a greater understanding of the relative dependence of emissions on load versus engine transients. These data are indicative of the type of investigations made possible by the development of this novel laboratory.

1. Introduction

In a recent critical review, Lloyd and Cackette (*1*) point out the scarcity of data for diesel emissions as compared with gasoline vehicles. Knowledge about the emissions from heavy heavy-duty diesel trucks (HHDDT) (gross vehicle weight > 33 000 lbs) is critical considering they contribute a disproportionate fraction of the NO_x and particulate matter (PM) emissions in many nonattainment areas relative to their population (*2*–*4*). For example, HHDDTs comprise only 2% of the total vehicles on the road but contribute to 60% of on-road mobile source primary PM emissions (*2*).

Even scarcer than information on regulated emissions from heavy-duty diesel (HDD) engines are data on the speciated emissions of volatile and semivolatile organic compounds (VOCs and SVOCs) and the physical and chemical nature of diesel PM. Diesel exhaust is a complex mixture comprised of thousands of constituents, including species known to be harmful to human health (*1*). The California Air Resources Board (ARB) defined diesel exhaust as a toxic air contaminant in 1998 (*4*). The International Agency for Research on Cancer (IARC) classified diesel exhaust as a probable human carcinogen (*5*). In 2002, the EPA released a health assessment document on the effects of diesel exhaust that stated: "Available evidence indicates that there are human health hazards associated with exposure to diesel exhaust" (*6*). The Multiple Assessment of Toxic Emission Sources Study (MATES) (*7*) identified diesel PM as the largest single source of carcinogenic PM in Southern California. Other toxic compounds in diesel exhaust listed in the MATES study include formaldehyde, 1,3-butadiene, benzene, toluene, ethylbenzene, and xylenes. The EPA has identified a number of hazardous air pollutants and published a list of 33 important Mobile Source Air Toxics (MSATs) (*8*). In addition to health impacts (*9*–*11*), PM emitted from diesel vehicles can reduce visibility due to direct light absorption by elemental carbon (EC) and light scattering (*12*–*14*).

Multiple investigators have reported the emissions of toxic compounds from diesel engines (*15*–*21*). However, no one has sampled the whole exhaust of a moving vehicle equipped with a HDD engine. Measurements of the emission rates for air toxics and PM are necessary to improve current emission inventories and modeling and to explore the effects of future emission control technologies.

The design of a PM sampling system raises a number of technical issues. Kittelson and others have pointed out the shortcomings of using forced dilution systems as compared with natural dilution systems (*22*, *23*). For example, hydrocarbon partitioning, nucleation, and coagulation processes that occur in the exhaust stream and sampling line will be affected by the dilution method, but the chemical composition of the exhaust will not be greatly affected. Despite the caveats raised, dilution tunnels remain the sampling system with the most repeatability and reliability and are specified by the EPA for the certification of diesel engines (*24*).

With the current emphasis on reducing emissions from HDD engines, more efforts are being undertaken to measure and understand in-use emissions. It is recognized that most available data on HDD emissions are generated from an engine on a laboratory test stand and that these data might not represent the emissions when the engine is part of a vehicle or another application. This paper describes the design and verification of the particulate and gas-phase toxics sampling systems installed within the mobile emissions laboratory (MEL) and presents first-time measurements of on-road HDD emissions with a full capture dilution tunnel system designed to meet the 2007 Code of Federal Regulations (CFR) (*24*).

---

* Corresponding author phone: (909) 781-5695; fax: (909) 781-5790; e-mail:dcocker@engr.ucr.edu.

† Department of Chemical and Environmental Engineering, Bourns College of Engineering.

‡ Bourns College of Engineering Center for Environmental Research and Technology.

10.1021/es049784x CCC: $27.50

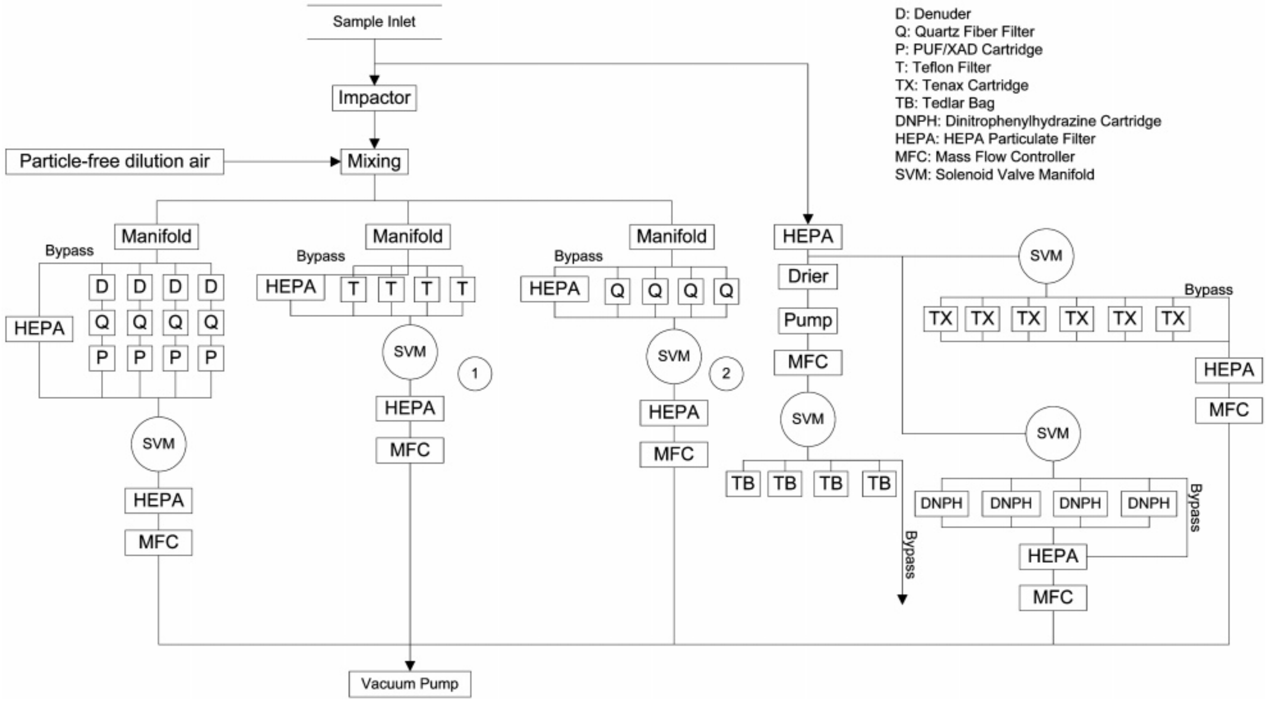

FIGURE 1. Detailed layout of the SDS.

2. Mobile Emissions Laboratory (MEL)

In an earlier publication, Cocker et al. (*25*) have described the design of an MEL for measuring regulated emissions in diesel exhaust. Briefly, the MEL design followed guidelines prescribed in the CFR (*24*) for certified emissions laboratory testing and included a dilution tunnel that captured the whole engine exhaust. The laboratory can be attached to an HHDDT for on-road emissions sampling or kept stationary for sampling of other emissions sources.

In Part I, we demonstrated the utility of measuring in-use emissions from HHDDTs as NO_x emission rates varied nonlinearly with fuel consumption rate due to changes in engine timing by the on-board electronic control module (ECM) (*25*). It was shown that the ECM would advance engine timing, leading to increased NO_x emission rates by as much as 3 times when compared with the fuel consumption rate. These nonlinearities were easily detected during on-road driving. The fraction of time spent off-cycle is a function of driving conditions. It is expected that nonlinearities in PM and toxic emission rates will also occur with advances/retardation of engine timing due to changes in the combustion process, which will lead to variations in OC composition. By testing emissions on-road, we can evaluate effects of ECM control on the measured emissions. Additionally, the effect of vehicle congestion, road-grade, altitude, wind, etc., can be monitored during on-road vehicular operation.

2.1. Secondary Dilution System (SDS) Overview. Early tests with the MEL sampled PM from the primary dilution tunnel; however, these tests resulted in a wide variation in the temperature of the filter face where PM was collected, and the temperature would occasionally exceed the 52 °C limit of the CFR (*24*). It is expected (*26*) that filter face temperature variations lead to changes in PM mass collected if a portion of the PM is semivolatile in nature. Furthermore, the revision of CFR for the year 2007 requires an SDS with control of the PM sample temperature to 47 ± 5 °C (*24*).

A detailed schematic and drawing of the SDS are presented as Figures 1and S1, respectively. The overall design is based on CFR 2007 guidelines (*24*) and includes sampling trains for collecting nonregulated gas-phase and semivolatile samples similar to that used by others (*15*−*21*). The SDS is designed to dynamically control both dilution air temperature and dilution ratio. Unit Series (Yorba Linda, CA) 7301 and 5301 mass flow controllers (MFCs) regulate flow rates throughout the SDS. To ensure sufficient mixing, the SDS sample probe is located >10 tunnel diameters from the initial mixing point of the primary dilution air with exhaust. Interchangeable probe tips allow for near-isokinetic sampling of PM from the primary dilution tunnel. The sample flow rate at the inlet of the secondary system can be adjusted up to 200 SLPM.

2.1.1. Size-Selective Impactor. For 2007, the CFR requires that a particle preclassifier with a 50% cut-point diameter between 2.5 and 10 μm be used prior to sample collection (*24*). An adjustable 31-jet impactor, based on the original design of Biswas and Flagan (*27*), was installed to remove PM larger than the CFR cut-point. Figure S1 (inset) contains a drawing of the impactor system. The PM cut-point at different flow rates can be varied by adjusting the length between the impaction plate and the nozzle exit and by using interchangeable nozzles.

2.1.2. Secondary Dilution Air Control and Mixing. Ambient air is used for dilution in the SDS after being compressed to 850 kPa using an Ingersoll Rand (Davidson, NC) OL5D5 oilless compressor and filtered with an Ingersoll Rand HE40 oil and particle filter. The dilution air is further dried with an Ingersoll Rand Dry Star DS25 refrigerated drier to a dew point of 0.5−4 °C at 850 kPa. The dilution air pressure is reduced to 178 kPa with an Ingersoll Rand 6ZC29A regulator and further dried to a dew point of −73 °C with desiccant. Remaining particulate is removed with a Gelman (Ann Arbor, MI) HEPA capsule. Unit Series 5301 MFCs regulate flow.

The dilution air passes through a coil of copper tubing (3.05 m × 1.27 cm o.d.), which is immersed in a Neslab (Union City, CA) RTE 211 refrigerated bath where the air is chilled to −15 °C. The cold, dry dilution air is heated with a Ni−Cr heating element to maintain a filter face temperature to 47 ± 5 °C using an Omega (Stamford, CT) i/32 temperature control unit. Conditioned dilution air radially enters a tubular sintered metal frit (100 μm stainless steel, Mott Corp., Farmington, CT) similar to that used in other sampling systems (*28*) (Figure S1). Exhaust sample enters the frit axially where it mixes with the dilution air. This dilution approach promotes turbulent mixing while minimizing thermophoretic losses to the walls.

2.2. Sampling and Analysis of PM. The SDS is designed such that multiple samples can be collected simultaneously. Three filter trains (may include annular denuders and polyurethane foam (PUF) cartridges) can sample simultaneously at predetermined flow rates (Figure 1). Four replicates of each filter train are available so that multiple modes can be sampled without operator intervention. Each sampling train is connected to a solenoid valve manifold and a MFC, all of which can be activated by the MEL's data acquisition system (*25*).

2.2.1. Total PM Mass. The filter weight procedure follows the guidelines of the CFR (*24*). Briefly, filters for the determination of total PM are collected on Pall Gelman (Ann Arbor, MI) 47 mm Teflo filters and weighed using a Cahn (Madison, WI) C-35 microbalance. Typical sampling flow rates range from 16 to 22 LPM, but can be adjusted from 3 to 30 LPM. Before and after collection, the filters are conditioned for 24 h in an environmentally controlled room (RH = 40%, $T = 25$ °C) and weighed daily until two weights within 3 μg are measured.

2.2.2. Elemental and Organic Carbon (EC-OC) Analysis. PM samples are also collected on 2500QAT-UP Tissuquartz Pall (Ann Arbor, MI) 47 mm filters that have been preconditioned at 600 °C for 5 h. A 1.5 cm^2 punch is cut out from the quartz filter and is analyzed with a Sunset Laboratory (Forest Grove, OR) Thermal/Optical Carbon Aerosol Analyzer according to the NIOSH 5040 reference method (*29*). A correction of 35% for OC gas-adsorption artifact is applied to the final OC. The correction factor is based on a comparison of OC captured on parallel quartz filters with one train containing an XAD-4 coated annular denuder for gas-phase semivolatiles upstream of the filter. Details can be found in ref *30*.

2.3. VOC Speciation. Samples for gas-phase chemical characterization are collected from the primary dilution tunnel. The sample is initially passed through a HEPA filter cartridge to remove PM. The flow is then split into two sample streams for the collection of carbonyls and light hydrocarbons (C_1-C_{12}). A schematic of this system can be seen in Figure 1.

2.3.1. Carbonyls. Carbonyls are collected on 2,4-dinitrophenylhydrazine (DNPH) coated silica cartridges (Waters Corp., Milford, MA). Samples of dilution air are also collected for background correction. A 0−1.0 LPM Unit Series 7301 MFC, solenoid valve manifold, and vacuum pump are used to draw a known volume of air through the DNPH cartridge. Sampled cartridges are extracted using 5 mL of acetonitrile and injected into a Shimadzu (Torrance, CA) high performance liquid chromatograph (HPLC) equipped with an SPD-10AV UV−vis detector. The HPLC sample injection, column, and operating conditions are set up according to the specifications of the SAE 930142HP protocol (*31*).

2.3.2. Detailed Light Hydrocarbon Composition. Samples for light hydrocarbon speciation are drawn from the primary dilution tunnel through a Nafion diffusion drier and Unit Series 7301 MFC with a diaphragm pump and are stored in opaque Tedlar bags. An additional bag of dilution air is collected for background correction. Within 4 h of collection, a sample from the Tedlar bags is injected into each of two HP 5890 Series II Plus gas chromatographs (GCs) with flame ionization detection (FID). The GC sample injection, columns, and operating conditions are set up according to the specifications of SAE 930142HP Method-1 and Method-2, for C_1-C_4 and C_4-C_{12} hydrocarbons, respectively (*31*). The original methods were designed and tested for analysis of vehicle tailpipe emissions from light-duty gasoline-powered engines and are easily applied to diesel exhaust measurements.

2.4. Other System Capabilities. The MEL is designed to collect substrates for complete chemical characterization of diesel exhaust. This paper focuses on nonregulated gas-phase compounds (including carbonyls), PM emission rates, and EC-OC carbon emission rates. Additional ports have been designed to collect samples using Tenax cartridges, impingers, annular gas-phase denuders, and PUF/XAD cartridges. Additional sampling ports are available to accommodate a condensation nucleus counter, scanning electrical mobility spectrometer, or any other constant flow instrumentation. The complete sampling system is shown in Figure 1, and details of these sampling systems will be provided in future publications.

3. Results and Discussion

3.1. System Verification. The repeatability of the MEL for the measurement of regulated gas-phase emissions was previously reported (*25*). Essentially, the MEL was able to accurately and repeatedly measure regulated gas-phase emissions from the primary dilution tunnel for various on-road driving cycles. Additionally, the emissions measured by the MEL were compared with the ARB heavy-duty chassis dynamometer facility at the Los Angeles Metropolitan Transportation Authority (MTA). In this paper, we demonstrate that the addition of an SDS allows the collection of high-quality data for PM and nonregulated emissions.

3.1.1. Dilution Factor Control. Propane, at >200 times ambient levels, was released into the primary tunnel and detected after dilution in the SDS. Propane recovery values over a dilution ratio (total tunnel flow:dilution air flow) range of 1−4.4 were within 2%. Figure S2 shows a range of propane recovery tests.

3.1.2. Control of the PM Filter Temperature. In addition to controlling the dilution air temperature, heat transfer losses from the SDS to the environment are minimized by placing the SDS in a heated chamber maintained at the desired sampling temperature. Figure S3 shows the temperature at the filter face and the mixing point of dilution air with exhaust gas over six consecutive runs of the creep phase of the ARB HHDDT cycle (*32*) and two consecutive runs of the transient phase of the HHDDT cycle, respectively. (See section 3.2 for details of the HHDDT cycle.) The location of the temperature sensors can be seen in Figure S1. This temperature control meets the 2007 CFR requirements for temperature control at the filter face (*24*).

3.1.3. On-Road Repeatability and Comparison of PM Mass between Parallel Samples. The reproducibility of parallel sampling and test-to-test repeatability of the SDS were tested on the ARB HHDDT cycle with a Freightliner tractor equipped with a model year 2000, 475 hp Caterpillar C-15 HDD engine using ultralow sulfur (<15 ppmw) diesel fuel. Two PM samples were collected in parallel to compare the reproducibility between sampling trains. These two sample trains are labeled 1 and 2 in Figure 1. Table 1 provides EC and OC emission rates (g mi^{-1}) during parallel sample collection and repeat tests for each of the four modes of the CARB HHDDT cycle. To collect a significant mass of PM on sample filters, three creeps were collected on each filter. The average difference between sampling channels was 1.2% for EC and 5.3% for OC. EC repeatability was 21.2%, 11.4%, 4.8%, and 3.6% for the cold-start idle, creep, transient, and cruise phase, respectively, while OC repeatability for the same four phases was 19.0%, 22.3%, 10.6%, and 5.4%, respectively.

3.1.4. Cross-Lab Correlation. A cross-lab correlation check was performed with the same Freightliner tractor at the ARB heavy-duty chassis dynamometer facility while operating on the hot urban dynamometer driving schedule (UDDS). Emission measurements were made using the MEL and ARB measurement benches on consecutive days. For these tests, the filter face temperature in the MEL was adjusted to 27 °C to match the ARB PM collection system. It should be noted that a retest on the chassis dynamometer with the MEL collecting emissions and the filter face temperature set

TABLE 1. Comparison of OC and EC Measurements of Parallel Sampling Trains[a]

		sample train 1		sample train 2	
	repeats	EC	OC	EC	OC
cold-start/idle (mg/min)	8	1.9 ± 0.2	42.3 ± 9.2	1.9 ± 0.6	42.8 ± 7.9
creep (mg/mi)	18	525 ± 57	436 ± 70	516 ± 66	437 ± 58.2
transient (mg/mi)	16	297 ± 21	175 ± 18	294 ± 22	174 ± 20
cruise (mg/mi)	8	81.9 ± 3.2	42.3 ± 0.7	79.2 ± 2.0	39.9 ± 2.7

[a] OC represents the mass carbon and has not been corrected for hydrogen or oxygen.

TABLE 2. Mass Emission Rates for Selected Species from an HHDDT Equipped with a CAT C-15 Engine (Model Year 2000)

	cold-start/idle (mg h^{-1})	creep (mg mi^{-1})	transient (mg mi^{-1})	cruise (mg mi^{-1})
PM	4494 ± 630	940 ± 185	449 ± 70.0	130 ± 1.6
EC	113 ± 24	520.3 ± 59.6	295 ± 14.3	80.6 ± 2.9
OC[a]	2458 ± 467	419.9 ± 93.5	174.4 ± 18.4	41.1 ± 2.2
formaldehyde	1487 ± 248.9	588 ± 34.5	115 ± 20.6	39 ± 2.0
acetaldehyde	438.2 ± 79.9	213.9 ± 14.6	37 ± 5.5	11 ± 0.4
total carbonyl	2150 ± 41.5	1082 ± 80.6	206 ± 31.6	60 ± 3.5
1,3-butadiene	37.9 ± 5.7	29.0 ± 2.0	6.3 ± 0.7	2.9 ± 0.5
benzene	50.3 ± 8.2	27.3 ± 2.5	6.2 ± 0.4	2.6 ± 0.8
toluene	36.5 ± 9.6	15.4 ± 1.8	2.4 ± 0.9	2.5 ± 1.1
ethylbenzene	6.8 ± 1.7	4.8 ± 1.1	1.1 ± 0.2	1.4 ± 0.3
o-xylene	14.0 ± 2.8	4.8 ± 3.1	0.7 ± 0.7	1.5 ± 0.7
m,p-xylene	17.9 ± 10.9	13.1 ± 4.8	2.0 ± 1.2	4.1 ± 1.7

[a] OC represents the mass carbon measured and is not corrected for hydrogen or oxygen content.

TABLE 3. Equivalent Miles Traveled during Transient Phase and Cruise Phase Operation Necessary To Match Emissions from 1 mi of Creep Phase Operation

	transient (mi)	cruise (mi)		transient (mi)	cruise (mi)
PM	2.1	7.2	1,3-butadiene	4.6	10.0
EC	1.8	6.5	benzene	4.4	10.5
OC	2.4	10.2	toluene	6.4	6.3
formaldehyde	5.1	15.1	ethylbenzene	4.5	3.5
acetaldehyde	5.7	18.8	*o*-xylene	7.1	3.1
total carbonyls[a]	5.3	18.0	*m,p*-xylene	6.5	3.2

[a] Total carbonyls represents the sum of 13 carbonyls detected in the SAE 930142 protocol (*28*).

to 47 °C recovered ~11% less PM mass than the test at 27 °C. Following triplicate tests, the MEL emissions data were submitted blind to ARB who provided the average percent differences between the labs for PM, CO, CO_2, NO_x, and total hydrocarbons (THC) as 0.1%, 18.4%, 2.7%, 8.0%, and 11.8%, respectively. A cross-lab check performed by other HDD laboratories reported similar deviations (*33*).

3.2. Examples of Mobile Sources with Standard Cycles. The recently released ARB 4-mode HHDDT test cycle simulates different driving conditions (*32*). The cycle consists of four modes: cold-start/idle, creep, transient, and cruise meant to represent idling, heavy congestion, arterial driving, and highway conditions, respectively. The vehicle speed versus time trace for the four-mode HHDDT driving cycle is presented in Figure S4.

Table 2 reports PM and some nonregulated gas-phase toxic emissions released from the Freightliner tractor (section 3.1.3) as it was driven on a road near sea level in Palm Springs, CA, following the ARB HHDDT driving cycle using CARB diesel fuel. The total gross vehicle weight of the MEL+ tractor was 60 000 lbs. It was found during this initial testing that DNPH cartridges (sampling from the SDS) were insufficiently loaded for proper analytical assessments. This was corrected by collecting subsequent samples from the primary dilution tunnel. The data presented in this paper include only those cartridges that were collected from the primary tunnel. All compound concentrations were well above those detected in dilution air (see Table S1).

Table 2 provides the emission rates for PM, EC, OC, and selected carbonyls and gas-phase toxics. Clear trends emerge from the data shown in Table 2 with respect to driving mode. For example, on a per mile basis, the creep mode has 7–15 times the emission rates of PM, formaldehyde, and benzene as in the cruise mode. A comparison of the emission factors of these compounds between modes clearly demonstrates the influence of driving cycle. Table 3 calculates the equivalent distance (in miles, for each pollutant) that the truck would have to travel in the transient and cruise modes to equal emissions from 1 mi in the creep mode.

Increases in the per mile emission rates for each of the compounds are due to a combination of several factors. Generally, the fuel consumed per mile is greatest for the creep phase and least for the cruise phase (3.2, 3.1, and 1.9 kg CO_2 mi^{-1} for the creep, transient, and cruise mode, respectively). However, even after normalization to CO_2 produced, the trend of higher emissions for creep versus cruise mode is maintained. In addition to higher fuel consumption, the engine spends a significant fraction of time at very low engine loads during the creep cycle, resulting in the engine operating at far from optimum conditions.

TABLE 4. Mass Emission Rates for Selected Species from a 350 kW BUG Equipped with a CAT 3406C Engine

	operation mode (% load, g phase^{-1}), duration (s)				
	10,[b] 500	25,[b] 500	50,[b] 500	75,[b] 450	100,[b] 400
PM	3.73 ± 0.14	3.35 ± 0.10	5.64 ± 0.17	8.01 ± 0.09	7.39 ± 0.81
EC	2.59 ± 0.17	2.31 ± 0.16	3.88 ± 0.35	4.76 ± 0.39	4.42 ± 0.16
OC	0.90 ± 0.06	0.82 ± 0.13	0.87 ± 0.23	1.67 ± 0.24	1.42 ± 0.54
formaldehyde	274 ± 54	256 ± 58	401 ± 54	624 ± 82	1077 ± 62
acetaldehyde	81.8 ± 8.6	73.8 ± 4.7	87.7 ± 6.9	115.5 ± 25.8	208.5 ± 33.0
total carbonyls[a]	466 ± 22	445 ± 59	596 ± 44	884 ± 138	1607 ± 177
1,3-butadiene	17.3 ± 1.1	13.2 ± 2.7	31.8 ± 9.9	36.6 ± 12.7	79.1 ± 23.0
benzene	38.9 ± 3.1	34.4 ± 3.5	39.2 ± 2.2	44.8 ± 3.1	101.4 ± 11.9
toluene	6.02 ± 1.59	5.90 ± 1.73	12.13 ± 1.71	13.77 ± 1.15	38.24 ± 1.37
ethylbenzene	3.65 ± 0.87	2.91 ± 1.43	3.45 ± 1.30	2.49 ± 1.26	3.40 ± 1.27
o-xylene	4.61 ± 0.75	4.06 ± 0.53	3.91 ± 1.64	3.98 ± 0.82	4.81 ± 0.37
m,*p*-xylene	2.34 ± 0.05	4.71 ± 1.06	5.34 ± 0.35	4.46 ± 0.96	10.80 ± 1.10
THC	2.93 ± 0.07	2.55 ± 0.04	2.26 ± 0.22	2.31 ± 0.55	3.69 ± 0.71
CH$_4$	0.25 ± 0.07	0.24 ± 0.03	0.56 ± 0.03	0.77 ± 0.12	1.40 ± 0.04
NMHC	2.71 ± 0.01	2.34 ± 0.07	1.78 ± 0.20	1.64 ± 0.44	2.48 ± 0.67
CO	14.12 ± 0.01	16.66 ± 0.27	47.07 ± 0.26	73.40 ± 0.33	66.07 ± 0.03
NO$_x$	57.5 ± 0.5	116.2 ± 2.7	229.7 ± 8.2	286.0 ± 1.4	295.6 ± 2.2
NO$_2$	4.36 ± 0.22	4.57 ± 0.45	8.64 ± 1.23	7.64 ± 1.50	14.00 ± 6.81
CO$_2$	6781 ± 16	11 040 ± 60	18 465 ± 55	24 006 ± 274	28 674 ± 508

[a] Total carbonyls represents the sum of 13 carbonyls detected in the SAE 930142 protocol (*28*). THC = total hydrocarbons, NMHC = nonmethane hydrocarbons. [b] 10%, 25%, and 50% loads were run for 500 s; 75% and 100% loads were run for 450 and 400 s, respectively.

The EC/OC ratio and PM emission factor are greatly affected by the driving mode. On a per mile basis, the creep mode had the highest PM, EC, and OC emission rates, while cruise mode had the lowest. The EC/OC ratio varied from 0.77 for the creep mode to 1.28 for the cruise mode. Thus, both PM, EC, and OC emission factors and EC/OC ratios are seen to vary with operating conditions. Sources of OC include unburned fuel oil, combustion byproducts, and lubricating oil (*23*, *34*), while the source of EC is fuel pyrolysis (*23*, *34*). It is impossible to determine the relative increase of each mechanism that occurs during the creep mode versus cruise mode without further chemical characterization of the organic fraction of the PM. The OC fraction increases during modes with low vehicle speed, while the EC fraction increases for modes at higher vehicle speed.

The findings presented in Table 3 have important implications in source apportionment and health risk assessments as EC is frequently used as a marker for diesel exhaust while the OC fraction is expected to contain many toxics. The data suggest that the largest health risk of diesel PM and gas-phase toxics will be during creep conditions in heavily congested areas. Accordingly, the results suggest that effective strategies to reduce the health risk of uncontrolled engines would be to either restrict truck traffic during congested conditions or install truck lanes to speed the flow of truck traffic.

3.3. Example of In-Use Emissions from Mobile Sources. Emissions from the Freightliner tractor (section 3.1.3) operating on CARB diesel fuel were measured for a trip on Interstate-15 from Riverside, CA to Victorville, CA. Specifics of this route are discussed in Cocker et al. (*25*). Briefly, this stretch of road is part of a major transportation corridor in the Los Angeles Basin and spans 53.2 mi, with an uphill grade of approximately 1.5% (net altitude gain of 1011 m) when traveling from Riverside to Victorville. Table S2 reports the total mass emissions from this trip for repeat runs in each direction. The driver followed another HHDDT on this trip. Test to test repeatability was high. The repeatability of parallel PM samples was within 3%, and the day-to-day variability was within 5% and demonstrates that the MEL can repeatedly monitor on-road emissions. The average PM emission rates of 171 mg mi^{-1} (uphill) and 134 mg mi^{-1} (downhill) most closely represent that of the cruise mode of the four modes of the ARB cycle (130 mg mi^{-1}). Differences seen in the uphill versus downhill transit through the corridor are explained by the relative power requirement (or fuel burned) for each direction. More details of the regulated emissions for this run can be found in Cocker et al. (*25*).

3.4. Example of a Stationary Source: Back-Up Generator (BUG). The MEL can also been used to characterize emissions from stationary sources such as diesel BUGs. Due to their close proximity to schools, hospitals, and municipal buildings, there is a great deal of interest in characterizing the emissions from BUGs. Emissions are measured by connecting the sample snorkel of the MEL to the exhaust pipe of the BUG. These units operate at constant engine speed in steady-state mode and are tested using the ISO 8178 Type D-2 cycle (*35*). The test cycle consists of operating the BUG at a constant engine speed at 10%, 25%, 50%, 75%, and 100% of the generator's maximum rated power output.

A 350 kW generator equipped with a CAT 3406C engine (model year 2000) was tested with CARB diesel fuel. Emissions are reported in Table 4 in g phase^{-1} for PM, EC, OC, carbonyls, and selected gas-phase species.

3.5. Comparison of BUG and HHDDT Emissions. The emissions from the BUG (section 3.4) can be compared with the Freightliner truck (section 3.1.3). Both engines have a displacement of 14.6 L and are based on the same engine block but have different fuel injectors, turbochargers, and air inlets. The BUG is designed for constant speed operation, while the C-15 engine in the Freightliner tractor is designed for transient operation.

In section 3.2, it was noted that the EC/OC ratio increased as the HHDDT was operated at higher sustained vehicle speeds (equivalent to less transient operations). Therefore, we expect that the BUG operating in steady-state mode would most closely emulate the cruise mode for the HHDDT. Figure 2 displays the EC/OC ratio for each operating mode of the BUG and the four modes of the ARB driving cycle. Analysis of the raw data showed that the difference in EC/OC ratio between the truck in the cruise mode and the BUG at any load point was due to both lower EC and higher OC for the truck. It is evident that the EC/OC ratio is not as dependent on engine load as compared with the transient operation of the engine. A larger data set of HHDDTs and BUGs is required to further assess these trends and will be a subject of a future paper.

The effects of the on-board ECM on NO$_x$ emission rates and fuel consumption were discussed in section 2. The integrated time spent in off-cycle engine operation was a

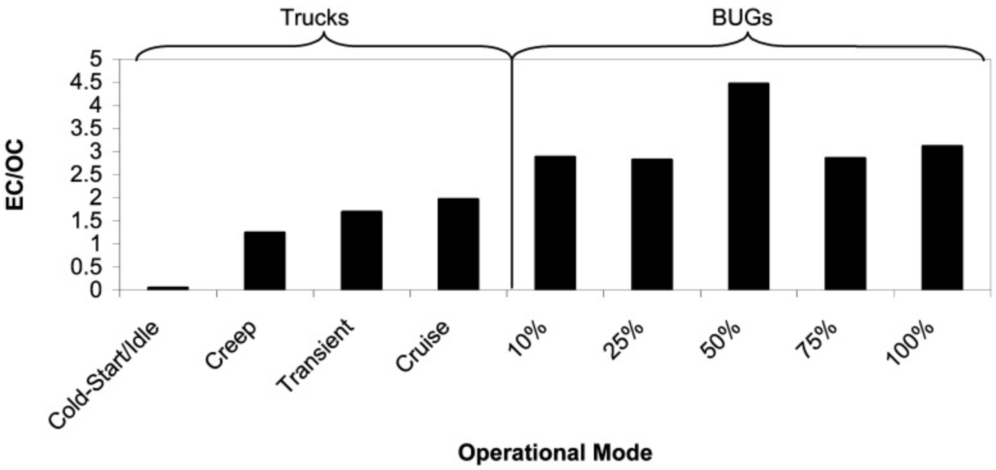

FIGURE 2. EC/OC ratios during different modes of operation for a truck tested over the CARB HHDDT cycle and a BUG tested over the ISO 8178 D2 cycle. OC represents the carbon content of the PM and has not been corrected for hydrogen or oxygen.

TABLE 5. PM/NO$_x$ Ratios

phase	PM/NO$_x$ (×100)
BUG	
10% load	6.49
25% load	2.88
50% load	2.46
75% load	2.80
100% load	2.50
HHDDT	
cold-start idle	2.74
creep	1.97
transient	2.15
cruise	0.61
Riverside to Victorville	0.76
Riverside to Victorville	0.73
Victorville to Riverside	0.85
Victorville to Riverside	0.73

function of the on-road driving conditions encountered and resulted in an increase of NO$_x$ emissions from 6.49 to 10.84 mg of NO$_x$ (g of CO$_2$)$^{-1}$ for transient and cruise modes. It is expected that as the NO$_x$ emissions rate increases, the PM emission rate will decrease (*36*). Table 5 compares the PM/NO$_x$ ratio for each of the five engine loads for the BUG, the four modes of the HHDDT ARB cycle, and the trips between Riverside and Victorville. In Table 5, we see that the PM/NO$_x$ ratio is fairly constant for the BUG in all modes other than the 10% load. On the other hand, the PM/NO$_x$ ratio varies across the four phases of the ARB HHDDT cycle.

The PM/NO$_x$ variability between the HDD engine and BUG is explained by differences in the transient nature of engine operation and fuel injection timing strategies: HHDDT engine ECMs are programmed with variable fuel injection timing, a feature not present in BUG engines. The high PM/NO$_x$ ratio seen at 10% load for the BUG is due to the engine operating far from its designed load. The variation of the PM/NO$_x$ ratio between the transient and cruise phases of the ARB HHDDT cycle may be explained by the observation that the cruise phase exhibited off-cycle operation more frequently than the transient phase (*25*). The PM/NO$_x$ ratio varies immensely between these two modes at 2.15 and 0.61 for the transient and cruise phases, respectively. The difference is due to both an increase in NO$_x$ emissions per fuel (67% increase) as well as a decrease in PM emissions per fuel (halved). Comparing these PM/NO$_x$ ratios to those obtained on the road between Riverside and Victorville (Table 5), we see that the values are most consistent with the ARB HHDDT cruise mode. Therefore, during transit between Riverside and Victorville, the off-cycle emissions as well as the transient nature of engine operation are well represented by the ARB HHDDT cruise mode. Further investigations of this phenomenon will be pursued in the MEL using a real-time particle sampler.

In Table 6, data sets obtained from the HHDDT and BUGs testing are compared on a per CO$_2$ basis (CO$_2$ can be used as a surrogate for fuel consumption). Clear differences are noted between emissions of different compounds when comparing the BUG and HHDDT emissions. Generally, the

TABLE 6. Mass Emission Rates Normalized by CO$_2$ Mass Emission Rate (g (kg CO$_2$)$^{-1}$)

	10	25	50	75	100	cold-start/idle	creep	transient	cruise
PM	0.55	0.30	0.31	0.33	0.26	0.43	0.18	0.14	0.07
EC	0.26	0.14	0.14	0.14	0.11	0.0109	0.068	0.063	0.028
OC	0.12	0.07	0.04	0.06	0.04	0.237	0.087	0.057	0.022
formaldehyde	40.41	23.19	21.72	25.99	37.56	143	110.6	35.6	19.9
acetaldehyde	12.06	6.68	4.75	4.81	7.27	42.26	40.2	11.5	5.6
total carbonyls[a]	68.72	40.31	32.28	36.82	56.04	207	203.6	63.8	30.6
1,3-butadiene[b]	2.55	1.20	1.72	1.52	2.76	3.66	5.46	1.95	1.48
benzene[b]	5.74	3.12	2.12	1.87	3.54	4.85	5.14	1.92	1.33
toluene[b]	0.89	0.53	0.66	0.57	1.33	3.52	2.90	0.74	1.28
ethylbenzene[b]	0.54	0.26	0.19	0.10	0.12	0.66	0.90	0.34	0.71
o-xylene[b]	0.68	0.37	0.21	0.17	0.17	1.35	0.90	0.22	0.77
m,*p*-xylene[b]	0.35	0.43	0.29	0.19	0.38	1.73	2.47	0.62	2.09
NO$_x$	8.48	10.53	12.44	11.91	10.31	15.8	8.98	6.49	10.84
THC	0.43	0.23	0.12	0.10	0.13	0.515	0.73	0.15	0.16

[a] Total carbonyls represents the sum of 13 carbonyls detected in the SAE 930142 protocol (*28*). THC = total hydrocarbons, NMHC = nonmethane hydrocarbons. [b] Reported in mg (kg CO$_2$)$^{-1}$.

emissions of carbonyls, gas-phase toxics, OC, and THC are higher for the more transient modes of the ARB HHDDT cycle, while the cruise phase emissions are more similar to the emissions of the steady-state operating BUG. The EC emission rate is significantly higher for this BUG as compared with the HHDDT. From Table 6, it is evident that the transient nature of on-road engine operation leads to more significant differences in per CO_2 emission rate than the variation in emissions between steady-state load points. For example, total carbonyls range from 32.3 to 68.7 mg of carbonyl (kg of $CO_2)^{-1}$ for the BUG and from 30.6 to 203.6 mg of carbonyl (kg of $CO_2)^{-1}$ for the three mobile phases of the ARB HHDDT cycle. The cold-start/idle emissions cannot be compared with BUG emissions because, as its name implies, the engine is warming and emissions at this stage will differ from those of a “hot” engine.

The effectiveness of the MEL in monitoring nonregulated emissions from mobile and stationary sources has been established. The MEL will be used to test a number of different emission sources, fuels, and operating conditions. Preliminary work shown in this paper clearly demonstrates the importance of on-road engine operation on the emission rates of PM and nonregulated gas-phase toxics for a single HHDDT. The relative emission rates on a per mile basis for each species increased dramatically as the vehicle was operated at lower speeds; this needs to be factored into health and source apportionment studies.

Acknowledgments

We wish to acknowledge Don Pacocha, Terry Traver, Kathalena Cocker, and Carlos Gaeta for their work in design and initial testing of the MEL. We also wish to acknowledge funding from the California Air Resources Board (ARB), U.S. Environmental Protection Agency (US EPA), California Energy Commission (CEC), South Coast Air Quality Management District (SCAQMD), Johnson Power Machinery, Ford Motor Co., International Truck & Engine, Mack Trucks Inc., and Volvo Truck Corp., Caterpillar Inc., Cummins Engine Co., and Detroit Diesel Corp.

Supporting Information Available

An AutoCad drawing of the SDS system (Figure S1), the results of a propane recovery test for the SDS (Figure S2), temperature traces for the SDS mixing point and filter face during on-road testing (Figure S3), and the ARB HHDDT four-mode speed trace (Figure S4); Table S1 with typical tunnel background values as a percent of measured values for each compound reported in this paper and Table S2 with regulated and PM emission values for the four runs between Victorville and Riverside. This material is available free of charge via the Internet at http://pubs.acs.org.

Literature Cited

(1) Lloyd, A. C.; Cackette, T. A. Diesel engines: environmental impact and control. *J. Air Waste Manage.* **2001**, *51*, 809−847.
(2) U.S. EPA. *National Air Pollutant Emission Trends Update, 1970−1997*; EPA 454/E-98-007; U.S. Government Printing Office: Washington, DC, 1998.
(3) U.S. EPA. Regulatory Announcement. EPA420-F-00-055; 2000.
(4) California Environmental Protection Agency. *Proposed Identification of Diesel Exhaust as a Toxic Air Contaminant: Part A. Exposure Assessment*; California Air Resources Board: Sacramento, CA, 1998.
(5) International Agency for Research on Cancer. *Diesel and Gasoline Engine Exhausts and Some Nitroarenes*; IARC Monographs 46 on the Evaluation of Carcinogenic Risks to Humans; Lyon, France, 1989.
(6) U.S. EPA. *Health Assessment Document for Diesel Exhaust*; Prepared by the National Center for Environmental Assessment; EPA/600/8-90/057F; Office of Transportation and Air Quality: Washington, DC, 2002.
(7) *Multiple Air Toxics Exposure Study (MATES-II) in the South Coast Air Basin*; Final Report. South Coast Air Quality Management District; March 2000.
(8) U.S. EPA. Technical Support Document. EPA420-R-00-023; December 2000.
(9) Pope, C. A.; Thun, M.; Namboodiri, M. M.; Dockery, D. W.; Evans, J. S.; Speizer, F. E.; Heath, C. W., Jr. Particulate air pollution as a predictor of mortality in a prospective study of U.S. adults. *Am. J. Respir. Crit. Care Med.* **1995**, *151*, 669−674.
(10) Dockery, D. W.; Pope, C. A.; Xu, X.; Spengler, J. D.; Ware, J. H.; Fay, M. E.; Ferris, B. G.; Speizer, F. E. An association between air pollution and mortality in six U.S. cities. *N. Engl. J. Med.* **1993**, *329*, 1753−1759.
(11) Vedal, S. J. Critical review-ambient particles and health: lines that divide. *Air Waste Manage.* **1997**, *47*, 551−581.
(12) Horvath, H. Atmospheric light absorption—a review. *Atmos. Environ.* **1993**, *27*, 293−317.
(13) Sloane, C. S.; Watson, J.; Chow, J.; Pritchett, L.; Richards, L. W. Size-segregated fine particle measurements by chemical species and their impact on visibility impairment in Denver. *Atmos. Environ.* **1991**, *25*, 1013−1024.
(14) Eidels-Dubovoa S. Aerosol impacts on visible light extinction in the atmosphere of Mexico City. *Sci. Total Environ.* **2002**, *287*, 213−220.
(15) Kweon, C. L.; Okada, S.; Foster, D. E.; Bae, M. S.; Schauer, J. J. Effect of engine operating conditions of particle-phase organic compounds in engine exhaust of a heavy-duty, direct injection (D.I.) diesel engine. *SAE Tech. Pap. Ser.* **2002**, *No. 2003-01-0342*.
(16) Schauer, J. J.; Kleeman, M. J.; Cass, G. R.; Simoneit, B. R. T. Measurement of emissions from air pollution sources. 2. C1 through C30 organic compounds from medium duty diesel trucks. *Environ. Sci. Technol.* **1999**, *33*, 1578−1587.
(17) . Hildemann, L. M.; Markowski, G. R.; Cass, G. R. Chemical composition of emissions from urban sources of fine organic aerosol. *Environ. Sci. Technol.* **1991**, *25*, 744−759.
(18) Lowenthal, D. H.; Zielinska, B.; Chow, J. C.; Watson, J. G.; Gautam, M.; Ferguson, D. H.; Neuroth, G. R.; Stevens, K. D. Differences in carbon composition of source profiles for diesel- and gasoline-powered vehicles. *Atmos. Environ.* **1994**, *28*, 731−743.
(19) McDonald, J. D.; Zielinska, B.; Sagebiel, J. C.; McDonald, M. R. Characterization of fine particle material in ambient air and personal samples from an underground mine. *Aerosol Sci. Technol.* **2002**, *36*, 1033−1044.
(20) Rogge, W. F.; Hildemann, L. M.; Mazurek, M. A.; Cass, G. R.; Simoneit, B. R. T. Sources of fine organic aerosol. 2. Noncatalyst and catalyst-equipped automobiles and heavy-duty diesel trucks. *Environ. Sci. Technol.* **1993**, *27*, 636−651.
(21) Gartziandia, E. L.; Tatry, V.; Carlier, P. Sampling and analysis of organic compounds in diesel particulate mater. *Environ. Monit. Assess.* **2000**, *65*, 155−163.
(22) Kittelson, D. B. Engines and nanoparticles: a review. *J. Aerosol Sci.* **1998**, *29*, 575−588.
(23) Abdul-Khalek, I. S.; Kittelson, D. B.; Brear, F. The influence of dilution conditions of diesel exhaust particle size distribution measurements. *SAE Tech. Pap. Ser.* **1998**, *No. 1999-01-1142*.
(24) Code of Federal Regulations. Protection of the Environment, 40 CFR 86.
(25) Cocker, D. R.; Johnson, K. J.; Shah, S. D.; Miller, J. W.; Norbeck, J. M. Development and application of a mobile laboratory for measuring emissions from diesel engines. I. Regulated gaseous emissions. *Environ. Sci. Technol.* **2004**, *38*, 2182−2189.
(26) Silvis, W. M.; Marek, G.; Kreft, N. Diesel particle measurement with partial flow sampling systems: a new probe and tunnel design that correlates with full flow tunnels. *SAE Tech. Pap. Ser.* **2002**, *SAE 2002-01-0054*.
(27) Biswas, P.; Flagan, R. C. The particle trap impactor. *J. Aerosol Sci.* **1988**, *19*, 113−131.
(28) Graze, R. R. Development and test of a fractional sampling system for diesel engine particulate measurement. *J. Eng. Gas Turbines Power* **1994**, *116*, 765−773.
(29) NIOSH. *NIOSH Manual of Analytical Methods*; National Institute of Occupational Safety and Health: Cincinnati, OH, 1996.
(30) Shah, S. D.; Cocker, D. R.; Miller, J. W.; Norbeck, J. M. Emission rates of particulate matter and elemental and organic carbon from in−use diesel engines. *Environ. Sci. Technol.* **2004**, *38*, 2544−2550.
(31) Siegl, W. O.; Richert, J. F. O.; Jensen, T. E.; Schuetzle, D.; Swarin, S. J.; Loo, J. F.; Prostak, A.; Nagy, D.; Schlenker, A. M. Improved emissions speciation methodology for Phase II of the Auto/Oil Air Quality Improvement Researh program—hydrocarbons and oxygenates. *SAE Tech. Pap. Ser.* **1993**, *No. 930142*.

(32) Gautam, M.; Clark, N.; Riddle, W.; Nine, R.; Wayne, W. S.; Maldonado, H.; Agrawal, A.; Carlock, M. Development and initial use of a heavy-duty diesel truck test schedule for emissions characterization. *SAE Tech. Pap. Ser.* **2002**, *No. 2002-01-1753*.

(33) Traver, M. L. *Interlaboratory Crosscheck of Heavy-Duty Vehicle Chassis Dynamometers. Final Report*; East Liberty, OH, May, 2002; CRC Project E-55-1.

(34) Abdul-Khalek, I. S.; Kittelson, D. B.; Graskow, B. R.; Wei, Q.; Brear, F. Diesel exhaust particle size: measurement issues and trends. *SAE Tech. Pap. Ser.* **1998**, *No. 980525*.

(35) International Organization for Standardization. ISO 8178-4, 1st ed.; 1996.

(36) Heywood, J. B. *Internal Combustion Engine Fundamentals*; McGraw-Hill: New York, 1988.

Received for review February 11, 2004. Revised manuscript received August 18, 2004. Accepted September 17, 2004.

ES049784X